

Effect of a milling cutter diameter on distortion due to the machining of thin wall thin floor components

Sridhar, G.^{a,*}, Ramesh Babu, P.^a

^aMechanical Engineering Department, University College of Engineering, Osmania University, Hyderabad, India

ABSTRACT

Machining of prismatic blocks, removing material up to 85 % on CNC machines to produce thin wall thin floor monolithic components replacing multi part assemblies has become common in aerospace industries. The greatest challenge when machining these components is part distortion. Selecting the right kinds of tools and machining parameters is of utmost importance in minimizing distortion. One of the important parameters is the size (diameter) of the cutter. Generally, within a production scenario, the selecting the size of the cutter is driven by the productivity and geometrical constraints of the component. Experience shows that selecting the wrong size of the cutter can lead to distortion and the selecting of a correct size of the cutter depends on heuristics. In order to understand the effect of cutter diameter on distortion, machining experiments were carried out by using different sizes of milling cutter, at constant feed, speed, depth of cut and volume of material removal rate, on a representative thin wall thin floor aluminium alloy (2014A T651) component, holding the part from the bottom, using a shop made vacuum fixture. Machining simulations were also carried out to understand the machining characteristics with any change in cutter diameter at constant feed, speed, depth of cut, and material removal rate. Experimental results show that the diameter of a milling cutter has an effect on distortion at constant feed, speed, depth of cut, and volume of material removal rate.

© 2015 PEI, University of Maribor. All rights reserved.

ARTICLE INFO

Keywords:

Milling
Thin wall thin floor
Distortion
Cutter size

*Corresponding author:

Garimella_s@yahoo.com
(Sridhar, G.)

Article history:

Received 28 December 2014
Revised 16 August 2015
Accepted 19 August 2015

1. Introduction

With recent increase in demand for more aircrafts and monolithic thin wall designs replacing complex assemblies for improving performance requirements, industries are facing a great challenge in machining thin wall components [1]. Machining these components comes with many challenges to achieve required design intent. One of the many problems encountered during manufacturing of these thin wall thin floor components is machining these parts with great accuracies without distorting the part after machining. Selection of right cutting parameters along with right kind of tool to machine these thin wall thin floor components is very important [2]. Attempt made in understanding the challenges in machining these thin wall thin floor components in the previous studies [3] and survey of the literature reveal that machining fixture scheme, cutting parameters, tool geometry, design features of the component etc., [4] all play a role in effecting the final distribution of residual stresses in turn effecting the distortion of the components. Total distortion problem right from design for distortion to manufacturing processes received great attention in research field for last fifteen years [5]. It was demonstrated by Hornbach and Prev y [6] that machining sequence plays an important role in distribution of residual stresses and optimizing the machining sequence will minimize distortion. Cui, Jung and

Moon [7] applied Taguchi method to know the effect of deformation caused by heat during cutting of aluminium alloy and found that cutting speed is the most influencing factor which causes deformation due to heat and the change of feed rate has an insignificant effect on heat deformation. Wang et al. [8] concluded that the main cause of thin walled machining distortion is due to redistribution of residual stresses during the machining process. Dong and Ke [9] verified with FEM and experiments that simulation can be done to select optimum tool path and machining sequences and avoid lengthy and expensive machining trials. Denkena and de León [10] conducted machining experiments and concluded that machining operations have influence on residual stress depth profile and showed a clear influence of residual stress distribution and part distortion on machining and tool parameters. Marusich et al. [11, 12] concluded that bulk residual stresses in the blank before machining along with the machine induced residual stresses influence distortion of the part. Bi et al. [13] proposed a simulation model taking into consideration cutting load, initial residual stresses, cutting sequence and tool path and predicted the result with an error of 19 % with experiments. Similar modelling and simulation method was proposed by Yang and Wang [14] for prediction and control of distortion. Belgasim and El-Axir [15] conducted machining experiments on aluminium magnesium alloy and observed that as per the process parameters the maximum residual stresses are either compressive or tensile, nose radius is sensitive to the residual stresses generation and feed rate is the most significant parameter affecting maximum residual stresses. Type of residual stress whether compressive or tensile depends on interfering effect of thermal and mechanical loads during machining. Izamshah et al. [16] conducted finite element analysis (FEA) and experimentation of thin walled component and proposed that FEA is an effective tool in predicting deflection and making error compensation to increase the accuracy of part eliminating expensive cutting trials. Chatelain et al. [4, 17] concluded with experiments that initial stresses embedded within the raw material has an effect on the final distortion of the component. The magnitude and distribution of the stresses effect the deformation size. Chantzis et al., [2] presented an industrial solution by first determining the initial residual stresses in the work piece, creating residual stress profiles and then optimizing the part location to minimize distortion. Songtao et al. [18] conducted machining experiment and established relationship among cutting parameters, cutting force and process deformation. They concluded that the machining deformation can be effectively controlled with combination of big radial cutting depth, small axial cutting depth at high spindle speed. Previous experimental studies conducted by authors, showed that there is significant effect of machining parameters particularly depth of cut and width of cut on distortion in machining thin wall thin floor aluminium components [19]. Huang et al. [20] conducted orthogonal experiments using high speed machining with four factors on aluminium alloy to find the residual stress distribution and concluded that decrease in cutting speed and increase in feed rate significantly increase compressive residual stresses increasing distortion. Tang et al. [21] concluded with their experiments that tool flank wear has a significant effect on residual stresses and increase in flank wear will shift from lower tensile or compressive stresses on the surface to tensile stresses. Increase in tool flank wear increases cutting forces and temperature. Xiaohui, et al. [22] concluded by conducting simulation and machining experiments that at smaller feed rate residual stresses are linearly proportional to uncut chip thickness in both tangential and radial directions and at higher feed rates only tangential residual stresses are in proportion to uncut chip thickness. They also concluded in their work to know the effect of tool diameter on residual stresses that large tool diameter will reduce uncut chip thickness and residual stress distribution is more uniform. In their experiments with 6 mm and 12 mm tools they found that maximum deformation value is reduced by 63.8 % with increase in tool diameter form 6mm to 12 mm and concluded that with further increase in diameter deformation still reduces [23]. Izamshah et al. [24] in their experimental studies on thin wall component found variation of deflection of wall with increase in helix angle of end mill.

Although some studies to understand, control and minimize machining distortion have been done by simulation and experiments, there is a lack of comprehensive study on the effect of machining distortion on machining and tool parameters which are assignable and controllable in a production shop. Hence, to study the effect of machining distortion on machining and tool pa-

rameters, attempts were made by authors in understand the challenge in machining thin wall thin floor components first [3] and carried out machining experiments to know the significance and effect of machining parameters using Taguchi experimental design [19]. It was found in a general production scenario that there is an inclination of selecting maximum size of cutter only taking geometry and accessibility into consideration, ignoring the distortion of the part caused by machining these slender thin wall thin floor components. Experience shows that machining these slender components using wrong size of cutter may distort the part. Knowing the effect of cutter size on distortion is important which will enable selection of suitable size of cutter to minimize machining distortion. So, in continuation of studies carried an attempt to understand the effect of cutter size on machining distortion keeping all machining parameters constant, a series of dry machining experiments were conducted with cutter sizes ϕ 6 mm to ϕ 16 mm which are generally used in production shops at constant material removal rate keeping all the other cutting parameters i.e., cutting speed, feed and depth of cut constant on aluminium alloy 2014A T651 used for producing avionic components, clamping the components on specially made vacuum fixture.

2. Experimental procedure

In order to find the effect of cutter size (diameter of milling cutter) on distortion of machining thin wall thin floor components, machining experiments were carried out on a representative part shown in Fig. 1.

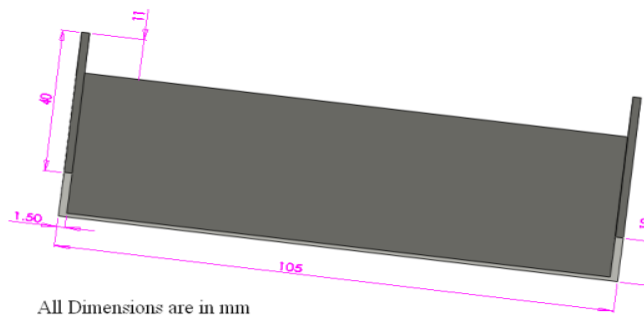


Fig. 1 Representative part used for experiments [19]

2.1 Work piece and material

The representative work piece was machined using aluminium alloy 2014 T651. This material is copper based alloy with high strength and excellent machining characteristics. The raw material was supplied as rolled plates with solution heat treatment and artificial age hardening subsequently stress relieved by stretching. This alloy is commonly used in many aerospace structural applications. The mechanical and chemical properties of the material are shown in Table 1 and Table 2 respectively. Blanks used for experiments were cut from plate with same heat number, sized to 105 mm \times 40 mm \times 12 mm on conventional milling machine and annealed to eliminate residual stresses within blanks.

Table 1 Mechanical properties of aluminium alloy AA2014 T651 [19]

Property	Value
Yield strength	380 MPa
Tensile strength	405 MPa
Hardness Rockwell B	82
Density	2.80 g/ cm ³
Poisson's ratio	0.2

2.2 Experimental setup

Machining experiments were carried out on 3-axis CNC vertical machining centre by holding the part from the bottom using a specially made vacuum fixture shown in Fig. 2. For consistency and to eliminate clamping effect work piece was held on the vacuum fixture as shown in Fig. 3. In total 18 random machining experiments (6 experiments with 3 replicates each) were carried by varying the diameter of milling cutter at constant cutting speed, feed per tooth, depth of cut and material removal rate. Material removal rate is calculated as given in Eq. 1, Eq. 2 and Eq. 3. Where N is Cutting speed in revolutions per minute, V_c is cutting speed in m/min, D is diameter of cutter in mm, F is feed in mm/min., F_t is feed per tooth in mm/tooth, n is number of flutes which is 2 in these experiments, DOC is depth of cut in mm, W is width of cut in mm and Q is material removal rate (MRR) in cm^3/min .

$$N = \frac{V_c \times 318.057}{D} \quad (1)$$

$$F = F_t \times n \times N \quad (2)$$

$$MRR (Q) = \frac{DOC \times W \times F}{1000} \quad (3)$$

Three samples were machined for each parameter and experiments were conducted randomly to reduce bias and to eliminate influence of extraneous variables during experimentation. The cutting tool path adopted for all the experiments was parallel spiral inside out as shown in Fig. 4. Width of cut is 70 % of the cutter diameter and the components were machined dry with out coolant. The cutting parameters used for experiments are shown in Table 3 and Table 4. The value of feed rate, speed and depth of cut selected were based on the available information in the factory manufacture and minimum cutter size used. The randomized experimental sequence, cutting parameters along with material removal rate is shown in Table 3.

Table 2 Chemical properties of aluminium alloy AA2014 T651 [19]

Property	Value (%)
Copper	3.8 to 4.8
Magnesium	0.2 to 0.8
Silicon	0.6 to 0.9
Iron	0.7 max
Manganese	0.2 to 1.2
Aluminium	Reminder



Fig. 2 Shop made vacuum fixture used for experiments [19]



Fig. 3 Work piece held on vacuum fixture

Table 3 Machining parameters with sequence of experiments

Sl. No.	Experiment No.	Cutter size D (mm)	Feed F (mm/min)	Speed N (rpm)	Width of cut W (70 % of D) (mm)	Material removal rate Q (cm ³ /min)
1	X22	8	955	4773	5.6	5.34
2	X31	10	764	3819	7	5.34
3	X13	6	1273	6364	4.2	5.34
4	X12	6	1273	6364	4.2	5.34
5	X61	16	478	2387	11.2	5.34
6	X23	8	955	4773	5.6	5.34
7	X51	14	546	2728	9.8	5.34
8	X42	12	637	3182	8.4	5.34
9	X33	10	764	3819	7	5.34
10	X53	14	546	2728	9.8	5.34
11	X63	16	478	2387	11.2	5.34
12	X62	16	478	2387	11.2	5.34
13	X43	12	637	3182	8.4	5.34
14	X11	6	1273	6364	4.2	5.34
15	X41	12	637	3182	8.4	5.34
16	X32	10	764	3819	7	5.34
17	X52	14	546	2728	9.8	5.34
18	X21	8	955	4773	5.6	5.34

Table 4 Cutting parameters

Parameter	Value
Feed/Tooth (F_t)	0.1 mm/tooth
Cutting speed (V_c)	120 m/min
Depth of cut (DOC)	1 mm
width of cut (W)	70 % of cutter diameter
Coolant	Dry machining

2.3 Machine tool and cutting tool

The machining experiments were carried out on Hardinge Bridgeport VMC 600 P3 3-axis vertical machining centre shown in Fig. 5 having maximum power of 13 kW and maximum spindle speed of 8000 rpm and the cutting tools used are 10 % cobalt two flute solid carbide slot drills of diameters 6 mm, 8 mm, 10 mm, 12 mm, 14 mm, and 16 mm with helix angle of 30° as shown in Fig. 6. Every experiment was carried out with new tool to avoid tool wear effect.

2.4 Distortion measurement

After conducting machining experiments, the distortion measurements were taken using Coordinate Measuring Machine (CMM), Metris LK Integra using CAMIO 4.4 software with specifications: size 800 mm × 700 mm × 600 mm, accuracy 1.9 + $L/450$ μm, repeatability 2.2 μm and probe error 3.6 μm. Fig. 7 shows the measurement being taken on CMM. Eighteen equally spaced similar points were marked on work piece by marking a grid as show in the Fig. 8 on opposite side to the face machined. Measurements were taken before machining on CNC and after machining and removal of work piece from the fixture on 18 similar points marked on each work piece. The difference in measurement before and after gives the distortion induced during machining [5]. Maximum deviation is taken for each work piece for distortion measurement as show in Fig. 9. The values of maximum measured distortion is given in Table 5. Apart from distortion, twist in the component after machining was also measured. Twist was measured as maximum lift in the edge of the component as shown in Fig. 10 using feeler gauge. The direction

of twist is shown in Fig. 11. Fig. 12 shows the lift produced because of twisting of the part. Maximum values of distortion and twist were used for comparison and analysis. The values of maximum measured twist is given in Table 6.

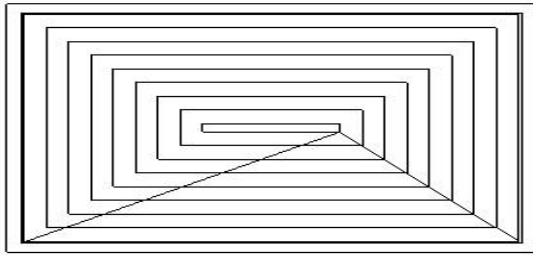


Fig. 4 Tool path layout [19]



Fig. 5 Hardinge Bridgeport VMC 600 P3



Fig. 6 Solid carbide slot drill

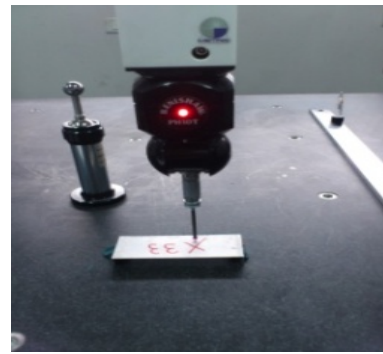


Fig. 7 CMM with work piece

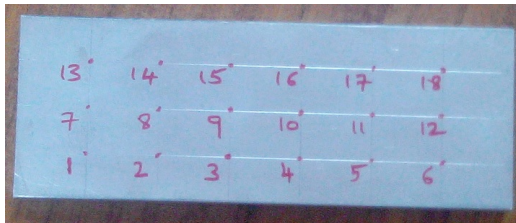


Fig. 8 Grid marking of measuring points

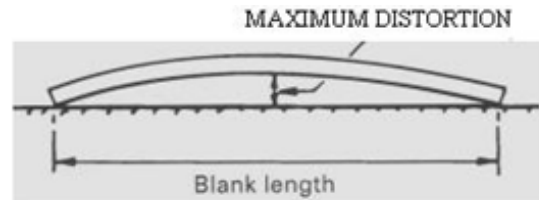


Fig. 9 Maximum distortion [19]

Table 5 Values of distortion achieved

Cutter size diameter (mm)	Distortion (mm)			
	Sample 1	Sample 2	Sample 3	Maximum
6	0.26	0.28	0.28	0.28
8	0.35	0.34	0.35	0.35
10	0.39	0.4	0.4	0.4
12	0.44	0.45	0.45	0.45
14	0.45	0.46	0.46	0.46
16	0.48	0.47	0.48	0.48

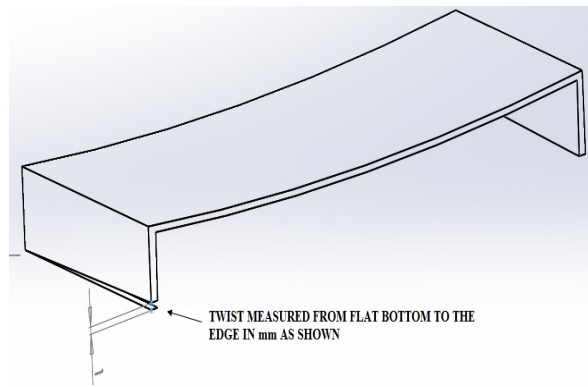


Fig. 10 Measurement of twist

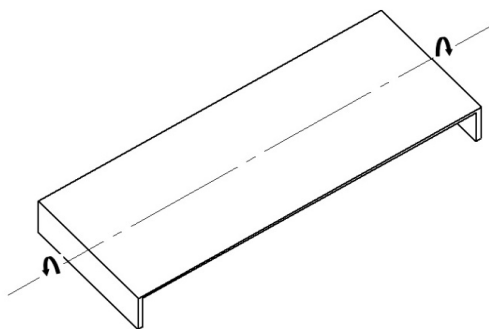


Fig. 11 Direction of twist

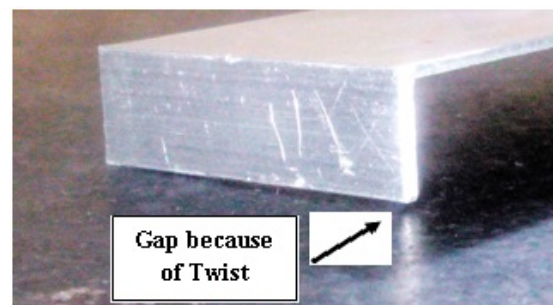


Fig. 12 Twist

Table 6 Values of twist achieved

Cutter size diameter (mm)	Twist (mm)			
	Sample 1	Sample 2	Sample 3	Maximum
6	0.29	0.3	0.3	0.3
8	0.53	0.5	0.52	0.53
10	0.78	0.8	0.77	0.8
12	0.86	0.9	0.89	0.9
14	0.98	0.99	0.97	0.99
16	1.05	1.03	1.05	1.05

2.5 FEM modelling for cutting characteristics

In order to understand the characteristics of machining aluminium alloy AA2014 T6, simulation experiments were carried at constant material removal rate, feed, speed and depth of cuts with varying milling cutter sizes, using commercial software Deform 3D. The tools and the work piece were modelled in SolidWorks and were imported to Deform 3D as .stl files. Fig. 13 shows the modelled tool. Simulations were carried using incremental Lagrangian formulation with implicit integration method. The solver used is conjugate-gradient with direct integration method. Oxley's equation to express flow stress relation is used for cutting simulation [25]. The material properties were taken from Deform 3D library. In these simulations the tool is defined rigid and is given thermal properties as it is much harder than work piece. The work piece is defined as plastic and was given both mechanical and thermal properties. Tetrahedron mesh is defined for both tool and work piece. Since milling involves high deformations at high strain rates, Deform3D uses adaptive meshing technique where in more elements are used at higher strain

rates and lesser elements at lower deformations for accuracy of solution [26]. Six runs of simulation were carried for various design of milling diameters keeping feed, speed, depth of cut and volume of material removal rate constant. In performing the simulation experiments small model of work piece is modelled for computational efficiency. Short material length of 1 mm at full width of cut defined for the cutter is chosen to save computational time without compromising the model integrity. Fig. 14 shows the milling simulation performed in Deform 3D. The instantaneous cutting force, temperature, and torque generated in simulation with stroke length are shown in Fig. 15. After simulation experiments, cutting characteristics i.e., average force in x, y, and z, average torque, average temperature and average heat flux were calculated with instantaneous simulation data for a cutter stroke of 1 mm at full width of cut. The average predicted values of cutting characteristics are given in Table 7.



Fig. 13 Modelled slot drill

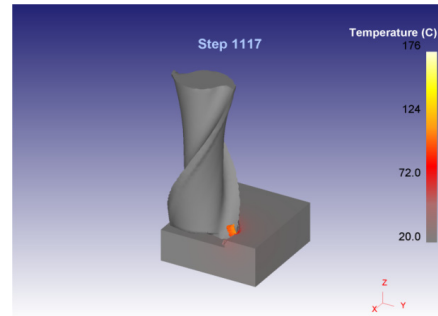
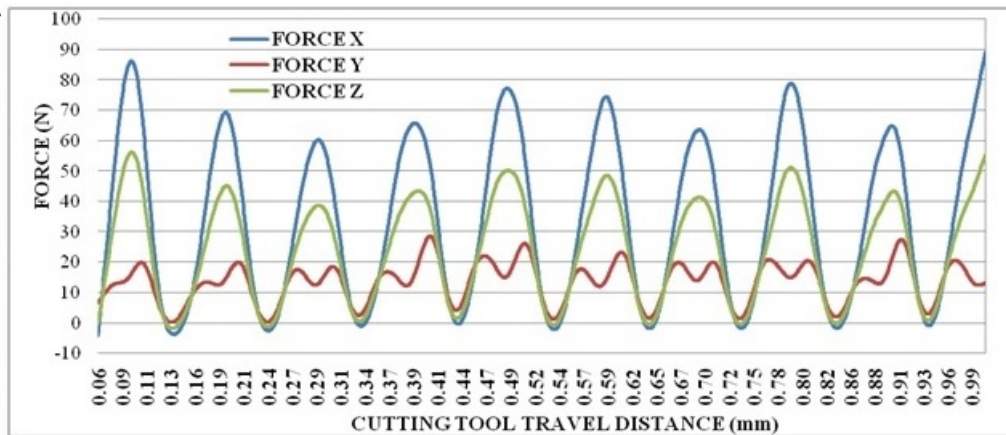
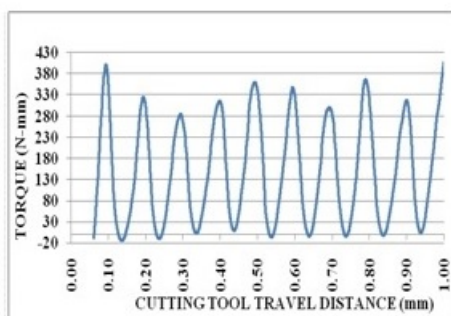


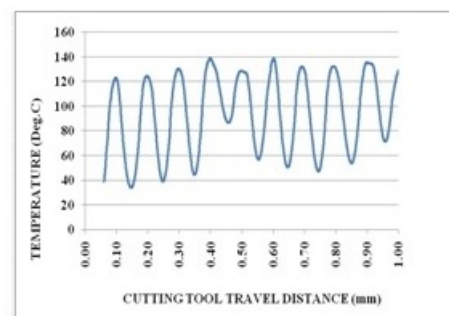
Fig. 14 FEM milling simulation using 8 mm slot drill showing transient temperature



a) Cutting forces in XYZ directions



b) Torque



c) Temperature

Fig. 15 Instantaneous predicted: a) Cutting forces, b) Torque, and c) Temperature generated with respect to stroke length of the cutter for 10 mm slot drill

Table 7 Simulated average predicted values of cutting characteristics

Diameter (mm)	Force (N)			Torque (N mm)	Heat flux (N mm/s)	Temperature (°C)
	X	Y	Z			
6	28.82	13.03	12.38	88.34	15033.29	92.87
8	28.13	11.19	15.62	111.94	14300.34	90.74
10	34.01	13.34	23.92	170.70	12298.63	98.62
12	32.22	13.13	27.56	195.62	10736.05	94.77
14	33.28	14.34	33.50	240.10	10536.05	102.15
16	34.01	15.02	39.33	281.51	10133.01	97.26

2.6 Chip length and chip thickness

Calculations were made to find the average chip thickness and chip length with increase in diameter of the cutter at constant feed, speed, dept of cut and material removal rates using Eq. 4 and Eq. 5 given by Martellotti [27, 28], where L_c is length of the chip in mm, D is diameter of the cutter in mm, a_e is width of cut mm, T is number of flutes, a_f is feed per tooth in mm/tooth and a_{avg} is average chip thickness in mm. The values of average chip thickness and chip length are shown in Table 8.

$$L_c = \frac{D}{2} \cos^{-1} \left(1 - \frac{2a_e}{D} \right) \pm \frac{a_f}{\pi D} T \left(\sqrt{(Da_e - a_e^2)} \right) \quad (4)$$

$$a_{avg} = \frac{a_f a_e}{L_c} \quad (5)$$

3. Results and discussion

After experiments, the effect of cutter size on distortion was evaluated by measuring the maximum distortion and twist in the components as shown in Table 5 and Table 6. To understand the cutting characteristics 6 simulation experiments were carried to evaluate average cutting forces, cutting temperature, torque and heat flux as shown in Table 7. To understand the chip characteristics, average chip length and chip thickness were calculated as shown in Table 8.

Table 8 Chip details

Diameter, D (mm)	Chip length, L_c (mm)	Average chip thickness, a_{avg} (mm)
6	5.98	0.07
8	7.96	0.07
10	9.94	0.07
12	11.92	0.07
14	13.91	0.07
16	15.89	0.07

Comparison of distortion and twist during machining is shown in Fig. 16. It could be observed from Fig. 16 and Table 5 that maximum distortion increased from 0.28 mm to 0.48 mm with increase in cutter diameter at constant feed, speed, depth of cut and material removal rate. It can also be observed from Fig. 16 and Table 6 that twist in the component increased markedly from 0.3 mm to 1.05 mm with increase in cutter diameter. Comparison of predicted cutting characteristics show marked increase in cutting forces in z-direction and torque with increase in cutter size from 6 mm to 16 mm as shown in Fig. 17 and Fig. 19, respectively. No significant increase in average cutting forces in x-direction and y-directions, and temperature as shown in Fig. 17 and

Fig. 18, respectively were noted. It is also observed that there is a slight decrease in heat flux with increase in cutter size as shown in Fig. 20. Calculations of chip length and chip thickness as in Table 8, show that, average length of chip increased with increase in cutter size and there was no change in average chip thickness.

The reason behind the increase in the deformation and twist with increase in cutter size with constant feed, speed, depth of cut and material removal rate is increase in torque and forces in z-direction. Further, it can be observed that there is an increase in average chip length effecting the temperature distribution indicating increase in time of contact per tooth with increase in cutter size, though there is no significant change in temperature generated during cutting. Hence, the results of experiments show that distortion of the component increase with increase in cutter diameter. So, minimum size of the cutter should be selected during machining of thin wall thin floor components to minimize distortion.

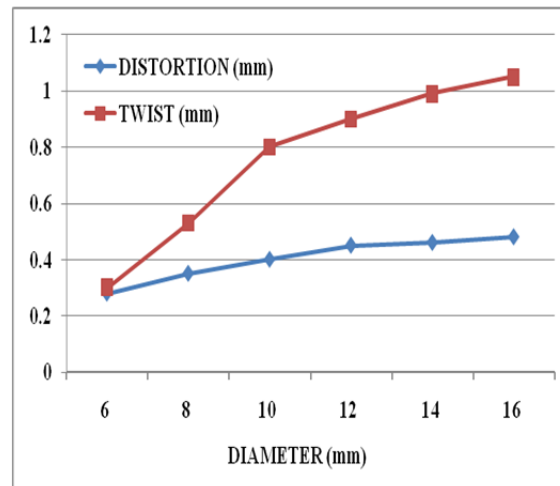


Fig.16 Distortion with change in cutter size

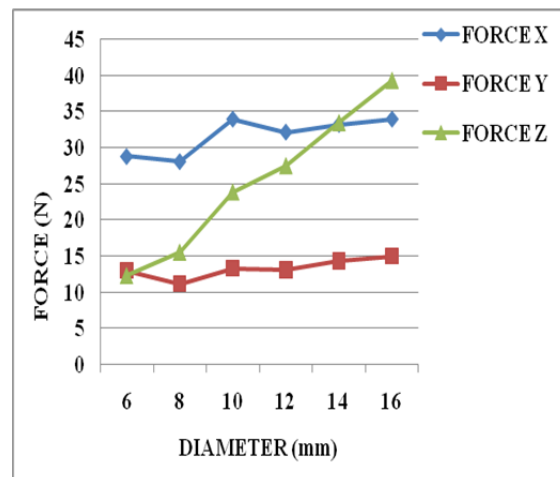


Fig. 17 Average predicted cutting forces with change in cutter size

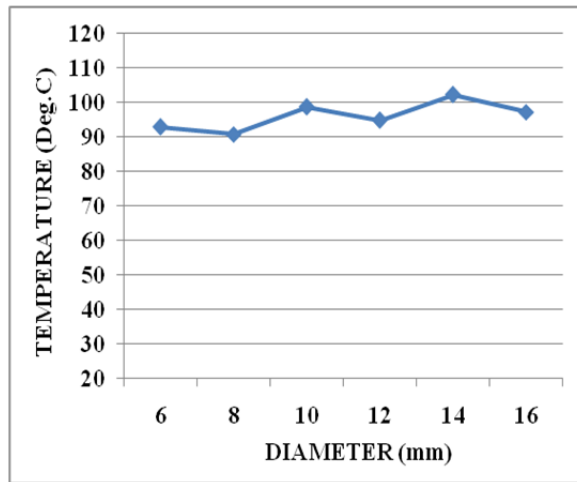


Fig. 18 Average predicted temperature with change in cutter size

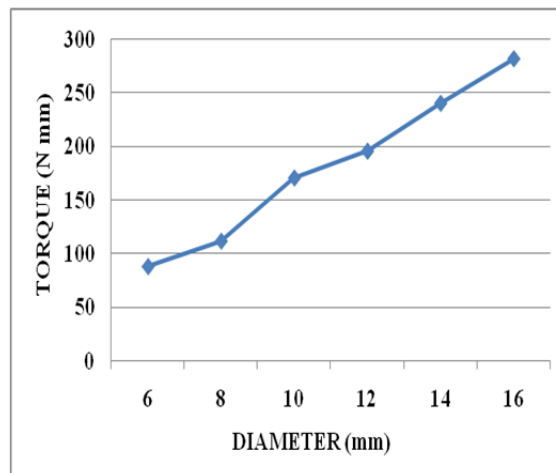


Fig. 19 Average predicted torque with change in cutter size

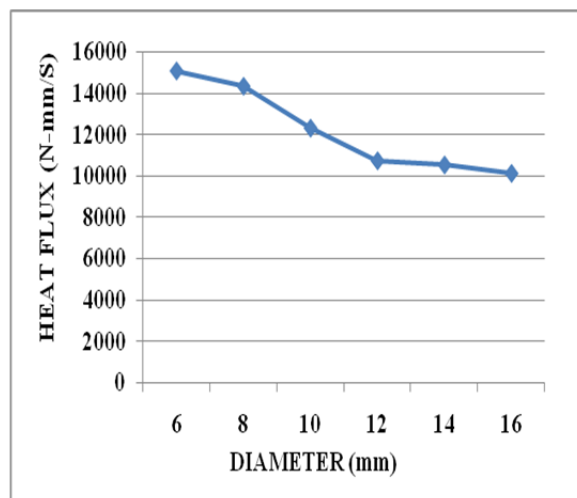


Fig. 20 Average predicted heat flux with change in cutter size

4. Conclusion

Machining experiments were conducted to know the effect of cutter size on distortion during machining. In the experimentation it is found that distortion increases with the cutter size at constant feed, speed, depth of cut and material removal rates. It is found from simulations, as the cutter size increases the forces in z-direction increase and play a dominant role in distorting the part and at larger cutter sizes twist in the machined part is more because of increase in cutting torque. So, precaution must be taken to see that smaller sizes of the cutter are selected for machining thin wall thin floor components to minimize distortion. Future work will focus on selection of tool geometry in terms of no. of flutes, right hand cutting, left hand cutting, helix angle and direction of helix angle and their effects on distortion.

Acknowledgement

The authors are thankful to the Head of Department, Osmania University for his constant encouragement and Support in smooth conduct of experiments. The authors are also thankful to the reviewers for their valuable inputs in enhancing the quality of the manuscript.

References

- [1] Sim, W.M. (2010). Challenges of residual stress and part distortion in the civil airframe industry, *International Journal of Microstructure and Materials Properties*, Vol. 5, No. 4-5, 446-455, doi: [10.1504/IJMMP.2010.037621](https://doi.org/10.1504/IJMMP.2010.037621).
- [2] Chantzis, D., Van-der-Veen, S., Zettler, J., Sim, W.M. (2013). An industrial workflow to minimise part distortion for machining of large monolithic components in aerospace industry, *Procedia CIRP*, Vol. 8, 281-286. doi: [10.1016/j.procir.2013.06.103](https://doi.org/10.1016/j.procir.2013.06.103).
- [3] Sridhar, G., Babu, P.R. (2013). Understanding the challenges in machining thin walled thin floored avionics components, *International Journal of Applied Science and Engineering Research*, Vol. 2, No. 1, 93-100, doi: [10.6088/ijaser.020100010](https://doi.org/10.6088/ijaser.020100010).
- [4] Chatelain, J.F., Lalonde, J.F., Tahan, A.S. (2011). A comparison of the distortion of machined parts resulting from residual stresses within workpieces, In: *Proceedings of the 4th International Conference on Manufacturing Engineering, Quality and Production Systems (MEQAPS '11)*, Barcelona, Spain, 79-84.
- [5] Ma, K., Goetz, R., Srivatsa, S.K. (2010). *Modeling of residual stress and machining distortion in aerospace components*, ASM Handbook, ASM.
- [6] Hornbach, D., Prev y, P. (1998). Development of machining procedures to minimize distortion during manufacture, In: *Proceedings of the 17th Heat Treating Society Conference and Exposition: Heat Treating*, ASM, Ohio, 13-18.
- [7] Cui, H., Jung, J.Y., Moon, D.H. (2005). The selection of machining parameters to minimize deformation caused by heat, In: *Proceedings of the Fall Conference of Society of Korea Industrial and Systems Engineering*, Korea.
- [8] Wang, Z.J., Chen, W.Y., Zhang, Y.D., Chen, Z.T., Liu, Q. (2005). Study on the machining distortion of thin-walled part caused by redistribution of residual stress, *Chinese Journal of Aeronautics*, Vol. 18, No. 2, 175-179, doi: [10.1016/S1000-9361\(11\)60325-7](https://doi.org/10.1016/S1000-9361(11)60325-7).
- [9] Dong, H.Y., Ke, Y.L. (2006). Study on machining deformation of aircraft monolithic component by FEM and experiment, *Chinese Journal of Aeronautics*, Vol. 19, No. 3, 247-254, doi: [10.1016/S1000-9361\(11\)60352-X](https://doi.org/10.1016/S1000-9361(11)60352-X).
- [10] Denkena, B., de Le n, L. (2008). Machining induced residual stress in wrought aluminium parts, In: *Proceedings of 2nd International Conference on Distortion Engineering*, Bremen, Germany, 107-114.
- [11] Marusich, T.D., Stephenson, D.A., Usui, S., Lankalapalli, S. (2009). Modeling capabilities for part distortion management for machined components, from <http://www.thirdwavesys.com/>, accessed August 16, 2015.
- [12] Marusich, T.D., Usui, S., Marusich, K.J. (2008). Finite element modeling of part distortion, In: Xiong, C., Liu, H., Huang, Y., Xiong, Y. (eds.), *Intelligent robotics and applications*, Lecture notes in computer science, Vol. 5315, Springer, Berlin Heidelberg, 329-338, doi: [10.1007/978-3-540-88518-4_36](https://doi.org/10.1007/978-3-540-88518-4_36).
- [13] Bi, Y.B., Cheng, Q.L., Dong, H.Y., Ke, Y.L. (2009). Machining distortion prediction of aerospace monolithic components, *Journal of Zhejiang University SCIENCE A*, Vol. 10, No. 5, 661-668, doi: [10.1631/jzus.A0820392](https://doi.org/10.1631/jzus.A0820392).
- [14] Yang, Y., Wang, Y.L. (2010). Analysis and control of machining distortion for aircraft monolithic component aided by computer, In: *Information and Computing (ICIC), 2010 Third International Conference on Information and Computing*, IEEE, Vol. 3, 280-283, doi: [10.1109/ICIC.2010.256](https://doi.org/10.1109/ICIC.2010.256).
- [15] Belgasim, O., El-Axir, M.H. (2010). Modeling of residual stresses induced in machining aluminum magnesium alloy (Al-3Mg), In: *Proceedings of the World Congress on Engineering*, Vol. 2, London, UK, 1268-1273.
- [16] Izamshah, R.A., Mo, J., Ding, S.L. (2010). Finite element analysis of machining thin-wall parts, *Key Engineering Materials*, Vol. 458, 283-288, doi: [10.4028/www.scientific.net/KEM.458.283](https://doi.org/10.4028/www.scientific.net/KEM.458.283).
- [17] Chatelain, J.F., Lalonde, J.F., Tahan, A.S. (2012). Effect of residual stresses embedded within workpieces on the distortion of parts after machining, *International Journal of Mechanics*, Vol. 6, No. 1, 43-51.

- [18] Songtao, W., Minli, Z., Yihang, F., Zhe, L. (2012). Cutting parameters optimization in machining thin-walled characteristics of aircraft engine architecture based on machining deformation, *Advances in Information Sciences and Service Sciences*, Vol. 4., No. 10, 244-252, doi: [10.4156/AISS.vol4.issue10.29](https://doi.org/10.4156/AISS.vol4.issue10.29).
- [19] Sridhar, G., Ramesh Babu P. (2013). Cutting parameter optimization for minimizing machining distortion of thin wall thin floor avionic components using Taguchi technique, *International Journal of Mechanical Engineering and Technology*, Vol. 4, No. 4, 71-78.
- [20] Huang, X., Sun, J., Li, J., Han, X., Xiong, Q. (2013). An experimental investigation of residual stresses in high-speed end milling 7050-T7451 aluminum alloy, *Advances in Mechanical Engineering*, Vol. 5, doi: [10.1155/2013/592659](https://doi.org/10.1155/2013/592659).
- [21] Tang, Z.T., Liu, Z.Q., Pan, Y.Z., Wan, Y., Ai, X. (2009). The influence of tool flank wear on residual stresses induced by milling aluminum alloy, *Journal of Materials Processing Technology*, Vol. 209, No. 9, 4502-4508, doi: [10.1016/j.jmatprotec.2008.10.034](https://doi.org/10.1016/j.jmatprotec.2008.10.034).
- [22] Jiang, X., Li, B., Yang, J., Zuo, X.Y., Li, K. (2013). An approach for analyzing and controlling residual stress generation during high-speed circular milling, *The International Journal of Advanced Manufacturing Technology*, Vol. 66, No. 9-12, 1439-1448. doi: [10.1007/s00170-012-4421-8](https://doi.org/10.1007/s00170-012-4421-8).
- [23] Jiang, X., Li, B., Yang, J., Zuo, X.Y. (2013). Effects of tool diameters on the residual stress and distortion induced by milling of thin-walled part, *The International Journal of Advanced Manufacturing Technology*, Vol. 68, No. 1-4, 175-186. doi: [10.1007/s00170-012-4717-8](https://doi.org/10.1007/s00170-012-4717-8).
- [24] IZamshah, R., Yuhazri, M.Y., Hadzley, M., Ali, M.A., Subramonian, S. (2013). Effects of end mill helix angle on accuracy for machining thin-rib aerospace component, *Applied Mechanics and Materials*, Vol. 315, 773-777, doi: [10.4028/www.scientific.net/AMM.315.773](https://doi.org/10.4028/www.scientific.net/AMM.315.773).
- [25] Yanda, H., Ghani, J.A., Haron, C.H.C. (2010). Effect of rake angle on stress, strain and temperature on the edge of carbide cutting tool in orthogonal cutting using FEM simulation, *Journal of Engineering and Technological Sciences*, Vol. 42, No. 2, 179-194. doi: [dx.doi.org/10.5614/itbj.eng.sci.2010.42.2.6](https://doi.org/10.5614/itbj.eng.sci.2010.42.2.6).
- [26] Gardner, J.D., Vijayaraghavan, A., Dornfeld, D.A. (2005). Comparative study of finite element simulation software, Laboratory for Manufacturing and Sustainability, UC Berkeley: Laboratory for Manufacturing and Sustainability, from <http://escholarship.org/uc/item/8cw4n2tf>, accessed August 16, 2015.
- [27] Shaw, M.C. (2005). *Metal cutting principles*, 2nd edition, Oxford University Press, Oxford, UK.
- [28] Jain, K.C., Chitale, A.K. (2010). *Textbook of production engineering*, 2nd edition, PHI Learning Pvt. Ltd., Delhi, India.